Supplemental Materials

Molecular Biology of the Cell

Kim and Rice

Supplemental Figure 1

A

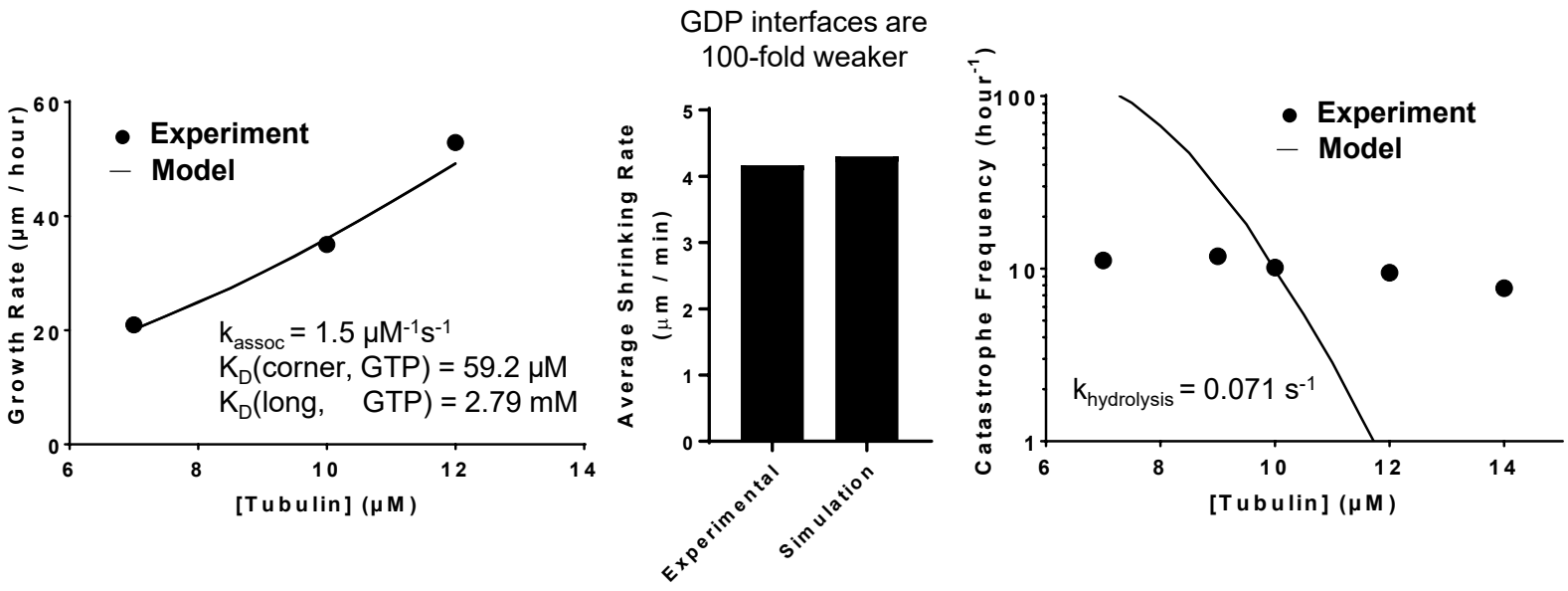

Supplemental Figure 1

Two state model trained to (Walker *et al.*, 1988) (**A**) Comparison between measured (black circles) and predicted (black line) growth rates. The two state model can recapitulate observed growth rates. (**B**) Comparison between measured and predicted shrinking rates. (**C**) Comparison between measured (black circles) and predicted (line) catastrophe frequency at different $\alpha\beta$-tubulin concentrations. The 2-state model cannot recapitulate the measured concentration-dependence of the catastrophe frequency.

Supplemental Figure 2

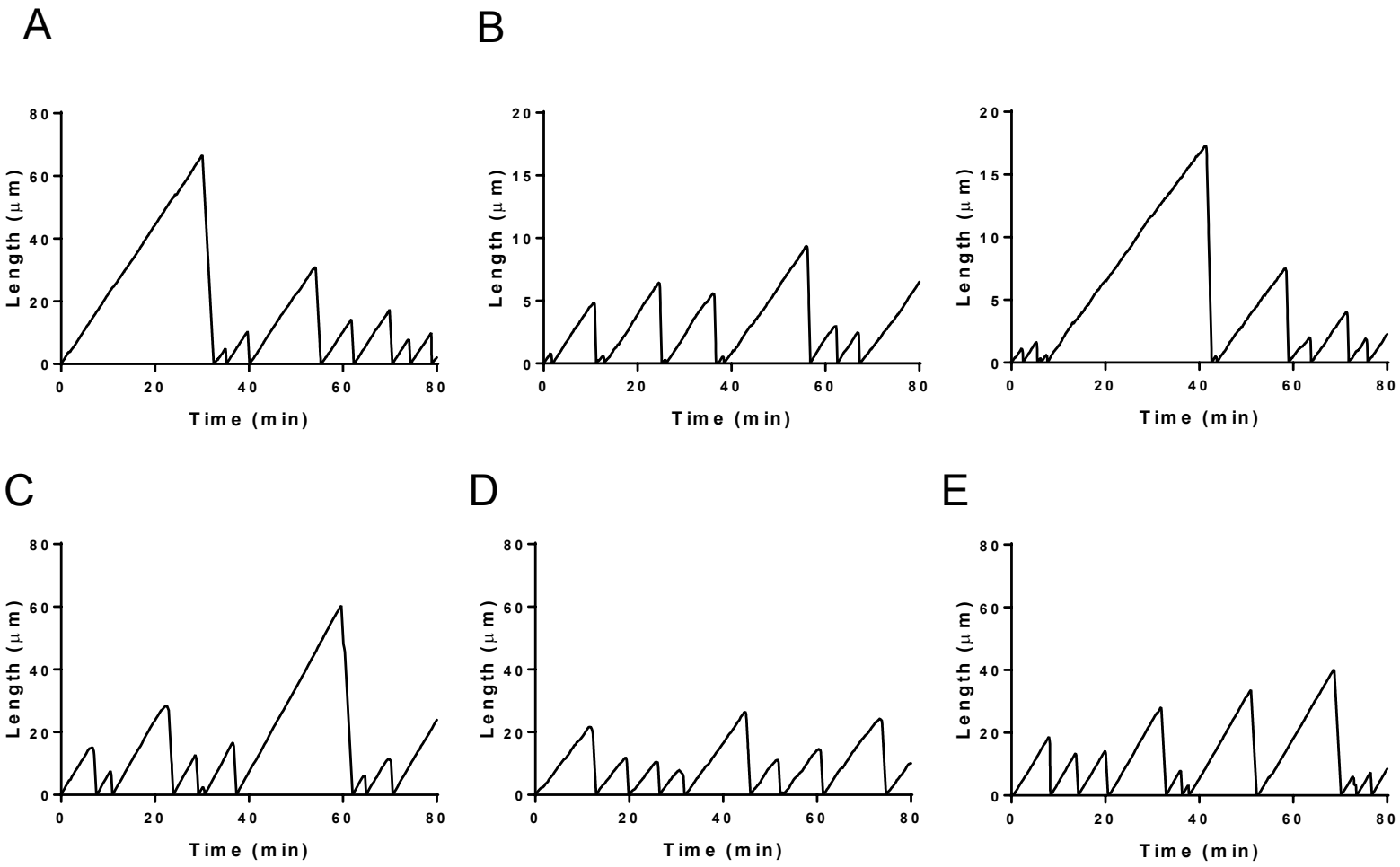

Supplemental Figure 2

Representative plots showing simulated MT length vs time. (**A**) Length vs time plot for the two-state model at 12 μM $\alpha\beta$-tubulin trained to (Walker *et al.*, 1988). (**B**) Length vs time plot of the two state model at 10 μM $\alpha\beta$-tubulin trained to (Gardner *et al.*, 2011b; Lawrence *et al.*, 2018). The y-axis is scaled differently compared to other panels in this figure because of the slower growth rates in this dataset. (**C**) Length vs time plot for the GDP.P_i model at 12 μM $\alpha\beta$-tubulin trained to (Walker *et al.*, 1988). In this model, the ratio between the hydrolysis rate and the phosphate release rates have been set to 1:1, and the strength of the longitudinal interface with GDP-P_i is as strong as the interface with GTP. (**D**) Length vs time plot for the long-range affinity modulation model at 12 μM $\alpha\beta$-tubulin trained to (Walker *et al.*, 1988). In this model, the neighbor influence range is 7, and the neighbor influenced affinity modulation is 90-fold. (**E**) Length vs time plot for the stimulated GTPase model at 12 μM $\alpha\beta$-tubulin trained to (Walker *et al.*, 1988). In this model the stimulated hydrolysis rate is 1000-fold faster compared to the random hydrolysis rate.

Supplemental Figure 3

A

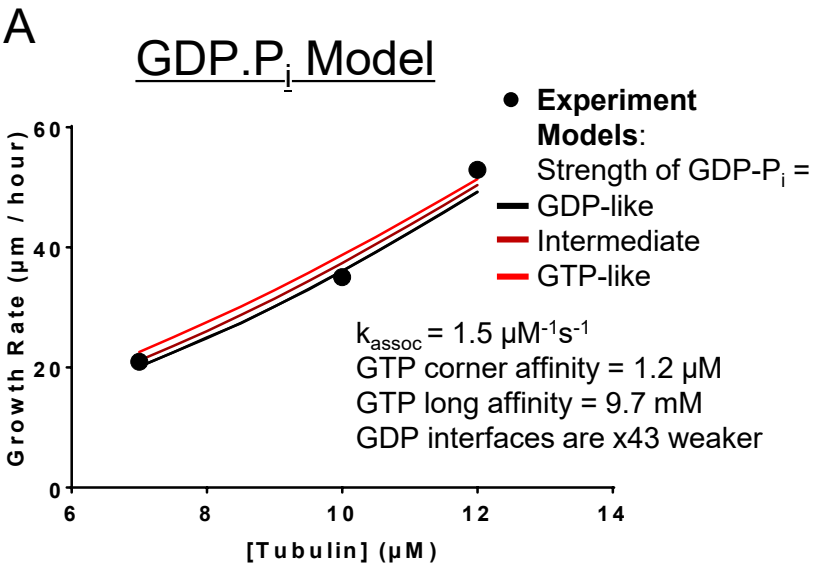

B

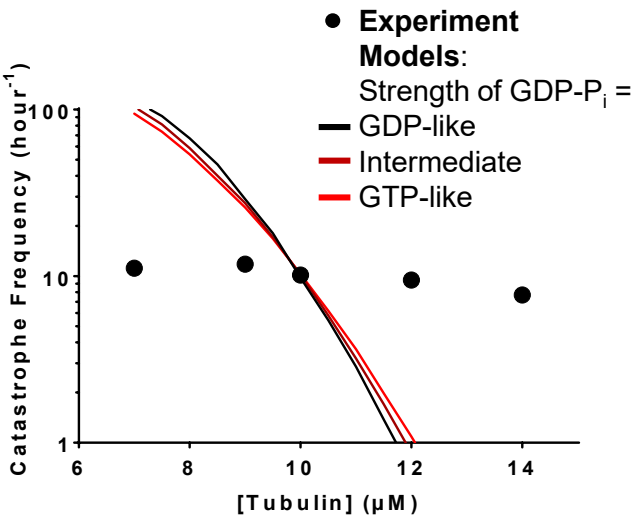

Supplemental Figure 3

GDP.P_i model trained to (Gardner *et al.*, 2011b; Lawrence *et al.*, 2018). (**A**) Comparison between measured (black circles) and predicted (black line corresponds to GDP.P_i interfaces having identical strength to GDP interfaces; red line corresponds to GDP.P_i interfaces having identical strength to GTP, brown line corresponds to GDP.P_i interfaces having intermediate strength) growth rates. All three scenarios can recapitulate observed growth rates. In this plot the ratio between the hydrolysis rate and the phosphate release rates have been set to 1:1. (**B**) Predicted catastrophe frequency as a function of concentration for different estimates about the strength of the GDP.P_i longitudinal interface. Varying the strength of the GDP-P_i interface has a limited effect on the concentration sensitivity of the catastrophe frequency. The ratio between the hydrolysis rate and the phosphate release rates have been set to 1:1. The GTPase rates are listed in Table 2.

Supplemental Figure 4

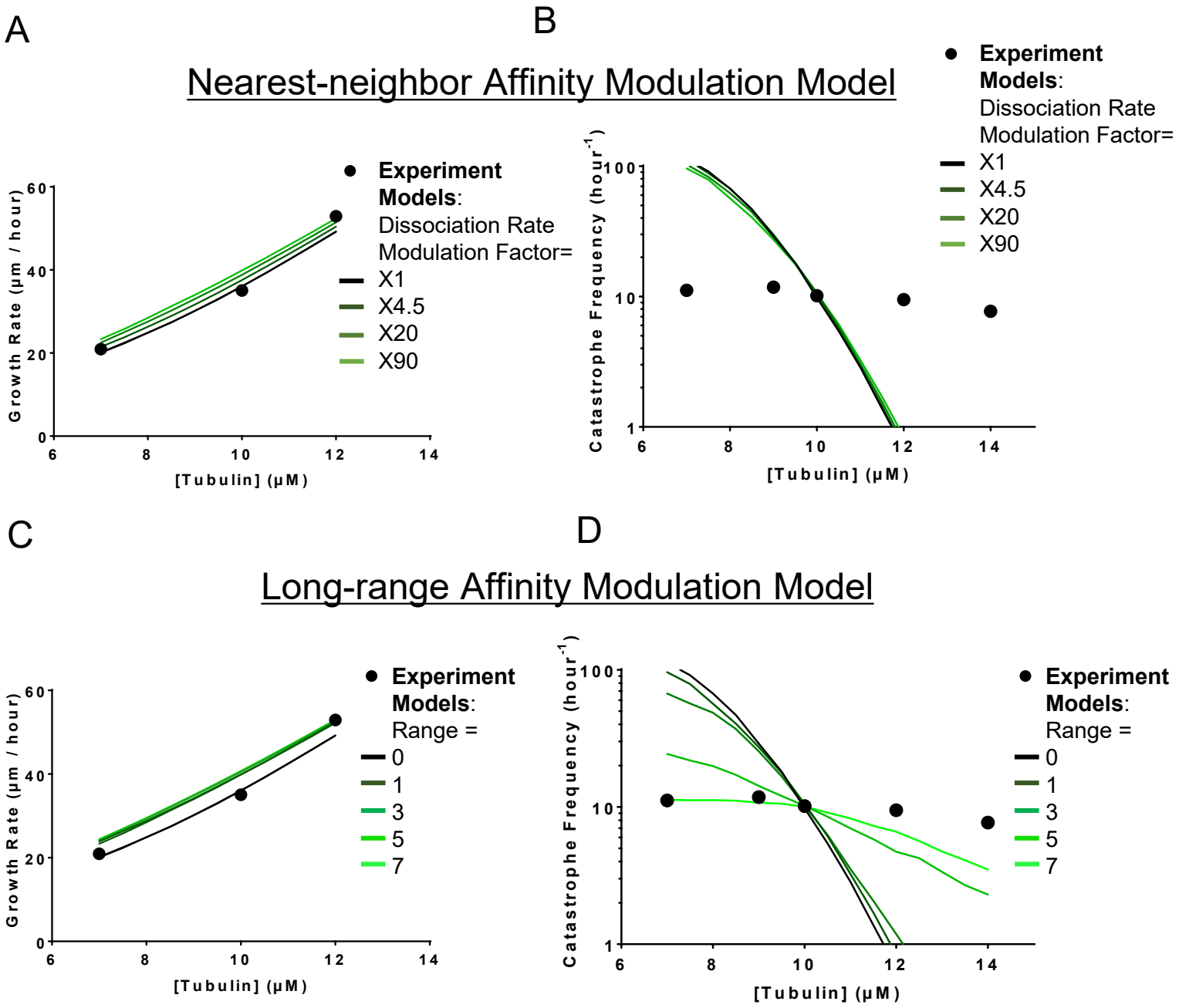

Supplemental Figure 4

Affinity modulation models trained to (Gardner *et al.*, 2011b; Lawrence *et al.*, 2018). (**A**) Comparison between measured (black circles) and predicted (blackest line corresponds to x1-fold increase in dissociation rates and the greenest corresponds to the x90-fold increase) growth rates, in the nearest-neighbor affinity modulation model. All four scenarios can recapitulate observed growth rates. (**B**) Predicted catastrophe frequency as a function of concentration for different fold-increases in $\alpha\beta$-tubulin dissociation rate. Varying the magnitude of $\alpha\beta$-tubulin dissociation modulation has a limited effect on the concentration sensitivity of the catastrophe frequency. (**C**) Comparison between measured (black circles) and predicted (blackest line corresponds to the modulation range of 0 and the greenest corresponds to the modulation range of 4) growth rates, in the long-range affinity modulation model. All five scenarios can recapitulate observed growth rates. In this plot the dissociation rate of the modulated $\alpha\beta$-tubulin is increased by 90-fold. (**D**) Predicted catastrophe frequency as a function of concentration for different maximum range of modulation. Varying the maximum range of modulation has significant effect on the concentration dependence of the predicted catastrophe frequency. The dissociation rate of the modulated $\alpha\beta$-tubulin is increased by x90-fold.

Supplemental Figure 5

A

B

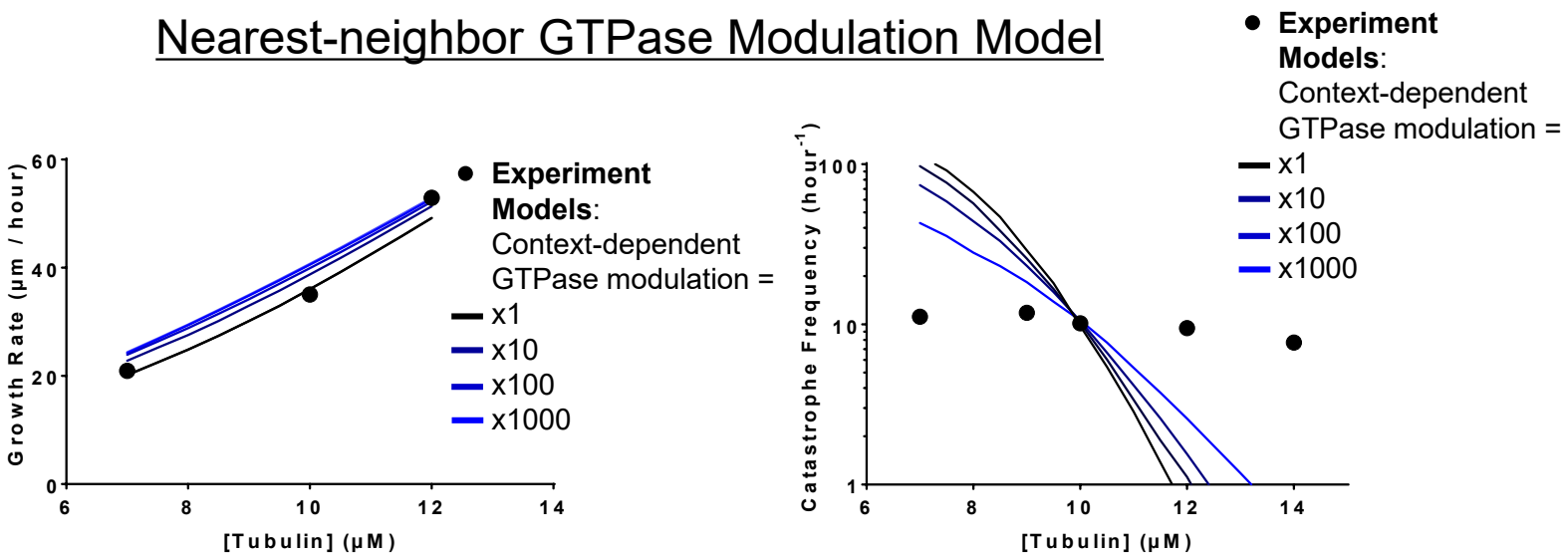

C

D

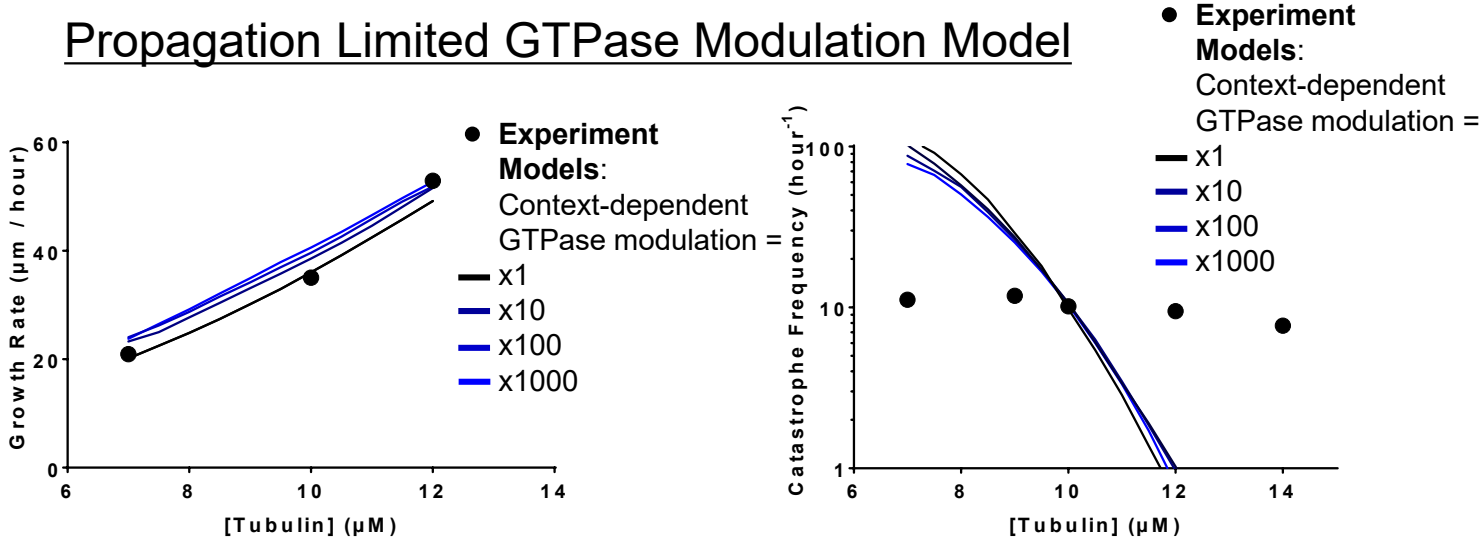

Supplemental Figure 5

GTPase modulation models trained to (Gardner *et al*., 2011b). (**A**) Comparison between measured (black circles) and predicted (blackest line corresponds to 1-fold increase in GTPase rates and the bluest corresponds to the 1000-fold increase) growth rates in the nearest-neighbor GTPase modulation model. All four scenarios can recapitulate observed growth rates. (**B**) Predicted catastrophe frequency as a function of concentration for different fold-increases in GTPase rate. Varying the magnitude of GTPase rate modulation has a significant effect on the concentration sensitivity of the catastrophe frequency. (**C**) Comparison between measured (black circles) and predicted (blackest line corresponds to 1-fold increase in GTPase rates and the bluest corresponds to the 1000-fold increase) growth rates, in the propagation-limited GTPase model. All four scenarios can recapitulate observed growth rates. (**D**) Predicted catastrophe frequency as a function of concentration for different fold-increases in GTPase rate, in the propagation-limited GTPase model. Limiting wave-like GTPase activity reverts the changes in predicted concentration dependence of catastrophe frequency observed in the original nearest-neighbor GTPase modulation model.

Supplemental Figure 6

A

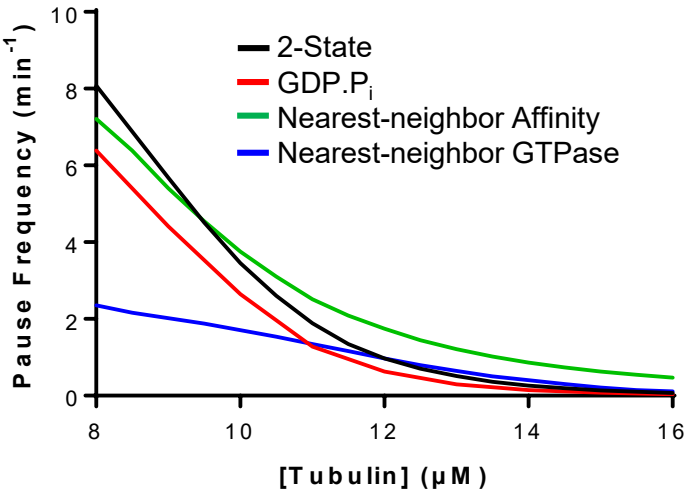

B

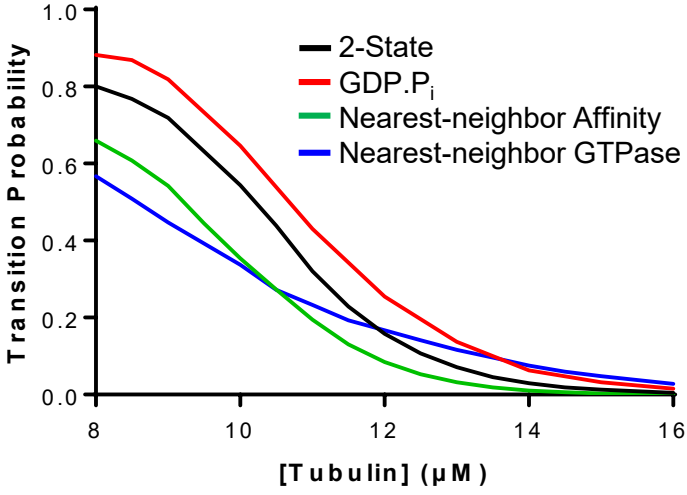

C

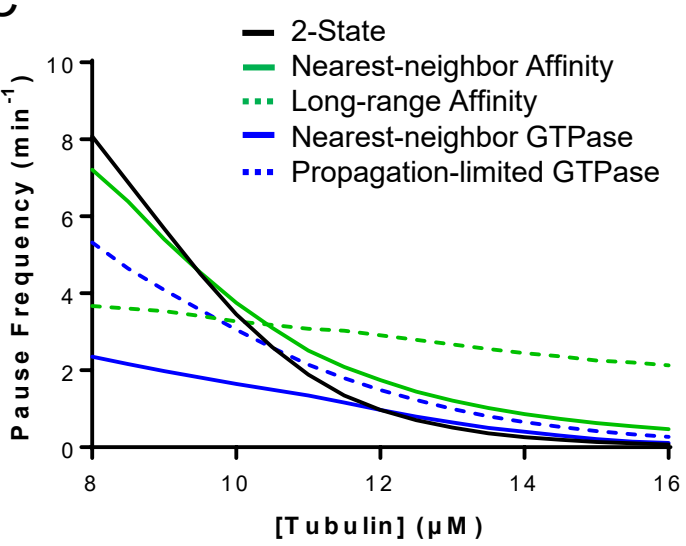

D

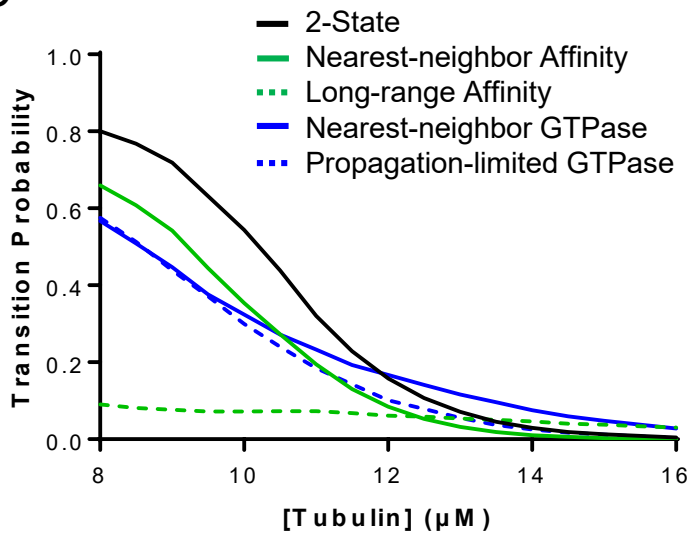

Supplemental Figure 6

Decomposition of catastrophe frequency. (**A**) The growth-to-pause frequency as the function of $\alpha\beta$-tubulin concentration of different models. The model parameters have been trained using (Walker *et al.*, 1988). (**B**) The pause-to-catastrophe frequency as the function of $\alpha\beta$-tubulin concentration of different models. (**C, D**) The growth-to-pause frequency and the pause-to-catastrophe frequency as the function of $\alpha\beta$-tubulin concentration of different models, showing the effects of long-range interactions. The solid lines represent models that were shown in (Supp. Fig. 6A-B). These models are shown here again for comparison.

Supplemental Figure 7

A

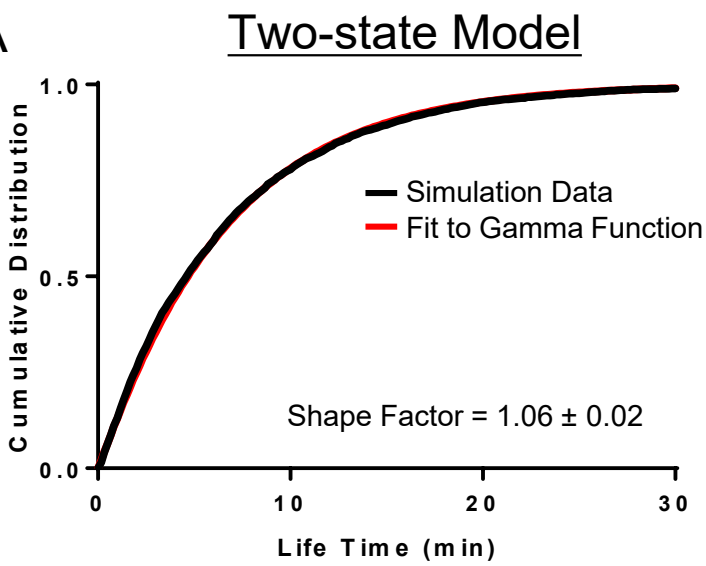

B

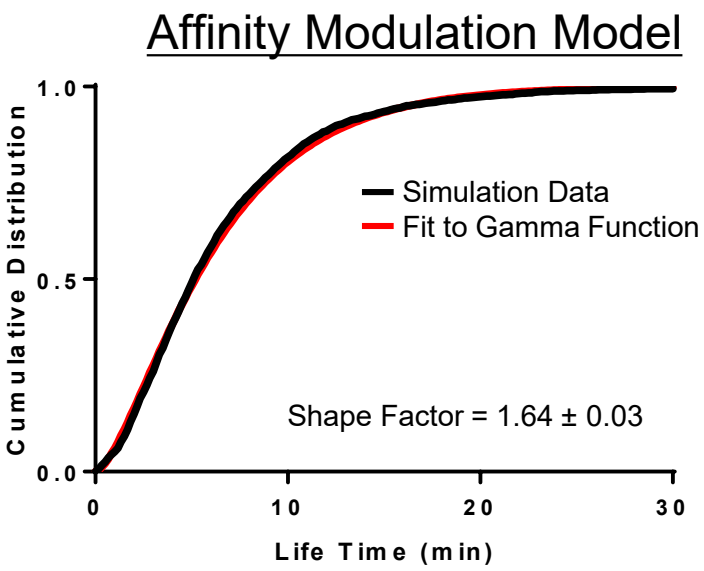

C

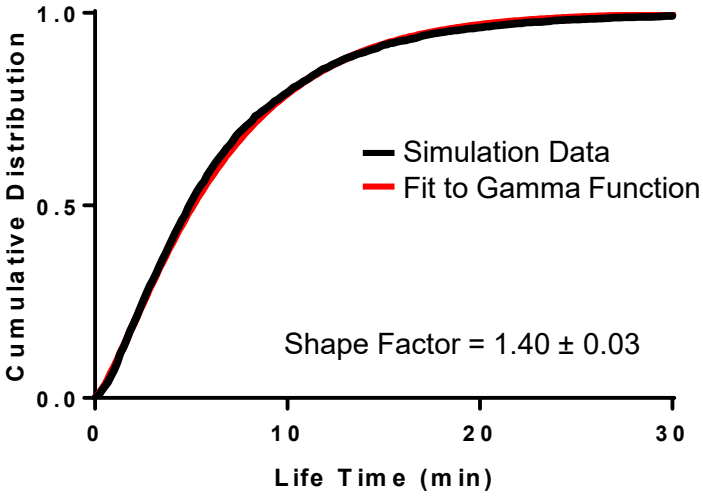

Supplemental Figure 7

The cumulative distributions of simulated MT lifetimes. (**A-C**) The cumulative distribution of (n = 4,000) MT simulations (black line) and their fits to the gamma distribution (red line) of different models. The model parameters have been trained using Walker et al data. The two state model shows no aging (shape factor = 1.05), while the affinity modulation model and the hydrolysis modulation model show small degree of aging, with the shape factors of 1.64 and 1.40, respectively.

Supplemental Table 1

A

k_{on}	2.0 s^{-1} μM^{-1}
ΔG^*_{long}	-7.00 k_BT
ΔG_{lat}	-6.86 k_BT
GDP-weakening factor	300

B

Hydrolysis Rates (s^{-1}) of GDP-P_i Model

Hydrolysis : Release	GTP-like	Intermediate	GDP-like
10:1	2.58	0.61	0.48
1:1	1.23	0.61	0.48
1:10	0.68	0.56	0.48

C

Hydrolysis Rates (s^{-1}) of Affinity Models

Dissociation Rate Modulation Factor	Basal GTPase Rate (s^{-1})
1	0.48
4.5	0.34
20	0.22
90	0.13

Range	Basal GTPase Rate (s^{-1})
0	0.48
1	0.13
3	0.036
5	0.016
7	0.006

D

Seam-crossing Allowed

GTPase Rate Modulation Factor	Basal GTPase Rate (s^{-1})
1	0.48
10	0.16
100	0.043
1000	0.0082

Seam-crossing **Not** Allowed

GTPase Rate Modulation Factor	Basal GTPase Rate (s^{-1})
1	0.48
10	0.20
100	0.081
1000	0.041

Supplemental Table 1

Parameters for models trained against the primary dataset (Walker *et al.*, 1988). (**A**) On-rate constant and strength of longitudinal and lateral interfaces. Here ΔG_{long} accounts for the entropic cost of losing rotational and translational degrees of freedom (see Methods), but ΔG_{lat} does not because it is treated as an 'add-on' interaction only. Thus, although the free energies for longitudinal and lateral interfaces appear similar, the longitudinal association is much higher affinity. The GDP weakening factor affects the longitudinal bond and is trans-acting (see Figure 1A). These values are used for all models. (**B**) GTPase rates used for GDP.P_i models. (**C**) GTPase rates used for the nearest-neighbor affinity modulation model (left) and for the long-range affinity modulation model (right). (**D**) GTPase rates used for nearest-neighbor GTPase modulation model (left) and for the propagation-limited GTPase model (right).

Supplemental Table 2

A

k_{on}	1.5 s^{-1} μM^{-1}
ΔG^*_{long}	-6.13 k_BT
ΔG_{lat}	-7.66 k_BT
GDP-weakening factor	100

B

Hydrolysis : Release

Hydrolysis Rates (s^{-1}) of GDP-P_i Model

	GTP-like	Intermediate	GDP-like
10:1	0.13	0.074	0.071
1:1	0.13	0.076	0.071
1:10	0.10	0.077	0.071

C

Hydrolysis Rates (s^{-1}) of Affinity Models

Dissociation Rate Modulation Factor	Basal GTPase Rate (s^{-1})
1	0.071
4.5	0.040
20	0.024
90	0.015

Range	Basal GTPase Rate (s^{-1})
0	0.071
1	0.015
3	0.0047
5	0.0017
7	0.0012

D

Seam-crossing Allowed

GTPase Rate Modulation Factor	Basal GTPase Rate (s^{-1})
1	0.071
10	0.030
100	0.010
1000	0.0025

Seam-crossing **Not** Allowed

GTPase Rate Modulation Factor	Basal GTPase Rate (s^{-1})
1	0.071
10	0.033
100	0.014
1000	0.0072

Supplemental Table 2

Parameters for models trained against the alternative dataset (Gardner *et al.*, 2011b; Lawrence *et al.*, 2018). (**A**) On-rate constant and strength of longitudinal and lateral interfaces. As in Supplemental Table 1, ΔG_{long} accounts for the entropic cost of losing rotational and translational degrees of freedom, but ΔG_{lat} does not. The GDP weakening factor affects the longitudinal bond and is trans-acting (see Figure 1A). These values are used for all models. (**B**) GTPase rates used for GDP.P_i models. (**C**) GTPase rates used for the nearest-neighbor affinity modulation model (left) and for the long-range affinity modulation model (right). (**D**) GTPase rates used for nearest-neighbor GTPase modulation model (left) and for the propagation-limited GTPase model (right).